Gas-phase interstitially modified intermetallics $R(Fe_{11}Ti)Z_{1-delta}$. II. 3d magnetization of the compounds $Y(Fe_{11}Ti)Z_{1-delta}$ (Z=N, C)

1992 J. Phys.: Condens. Matter 4 8209

(http://iopscience.iop.org/0953-8984/4/42/010)

J. Phys.: Condens. Matter 4 (1992) 8209–8220. Printed in the UK

Gas-phase interstitially modified intermetallics $R(Fe_{11}Ti)Z_{1-\delta}$: II. 3d magnetization of the compounds $Y(Fe_{11}Ti)Z_{1-\delta}$ (Z = N, C)

Qi-nian Qi, Y P Li† and J M D Coey
Department of Pure and Applied Physics, Trinity College, Dublin 2, Ireland

Received 6 April 1992

Abstract. The magnetization, Curie temperature and ^{57}Fe hyperfine fields are measured for $Y(Fe_{11}Ti)$ and the interstitial nitride and carbide. Data are compared with the results of electronic structure calculations by the OLCAO method. All compounds are weak ferromagnets. The increase of magnetization from 19.0 μ_B FU^{-1} in the parent compound to 21.6 μ_B FU^{-1} in the carbide and nitride is essentially due to volume expansion. A corresponding increase in average ^{57}Fe hyperfine field is observed in the nitride, but not in the carbide due to different 4s transferred hyperfine fields.

1. Introduction

In rare-earth–transition-metal intermetallic series, yttrium compounds are often studied in order to focus on the properties of the transition metal, since yttrium can be regarded as a non-magnetic rare earth having atomic radius similar to these of elements in the middle of the rare-earth series. Many electronic structure calculations are done for the prototype yttrium intermetallic compounds [1–3].

The recent discovery that the magnetic properties of iron-rich rare-earth intermetallics may be dramatically altered when nitrogen [4, 5] or carbon [6] is inserted into interstitial sites by gas–solid reaction (the *gas-phase interstitial modification* process) has led to investigations of the origin of the increase in iron magnetization and Curie temperature, and discussion of physical limits to such increases [7]. It was proposed at the outset, in view of the known pressure dependence of the magnetic properties of Y_2Fe_{17} [8], that the changes wrought by the interstitials are essentially due to magnetovolume effects on the iron d band. This view has been confirmed by electronic structure calculations on nitrides [9, 10] and carbides [11] with the 2:17 structure and nitrides with the 1:12 structure [12].

In our earlier paper, referred to as I [13], we have presented the magnetic properties of the $R(Fe_{11}Ti)C_{1-\delta}$ series with $\delta < 0.2$. Curie temperatures increase by about 160 K on carbonation, and there are some changes of magnetization. The effects are similar to those observed in the $R(Fe_{11}Ti)N_{1-\delta}$ series [14–16]. Here we focus on the iron magnetism, including Curie temperature, total magnetization and local

† On leave from: Department of Physics, University of Science and Technology of China, Hefei, People's Republic of China.

0953-8984/92/428209+12$04.50

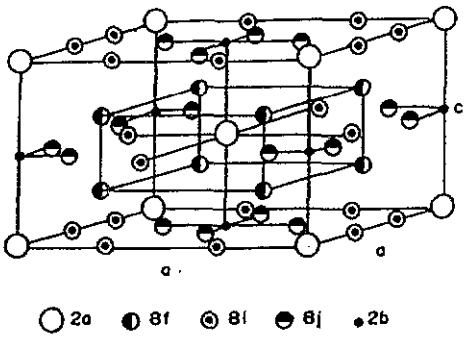

Figure 1. Crystal structure of $Y(Fe_{11}Ti)$ showing the 2b site interstitial occupied by N or C.

magnetization at the various atomic sites using experimental measurements (magnetization, ^{57}Fe Mössbauer spectroscopy) and electronic structure calculations (OLCAO) for $Y(Fe_{11}Ti)Z$. The $ThMn_{12}$ structure is illustrated in figure 1, including the 2b interstitial site occupied by nitrogen [17] or carbon. The pure iron end-members are unstable, and the Ti needed to stabilize the structure preferentially enters 8i sites [18].

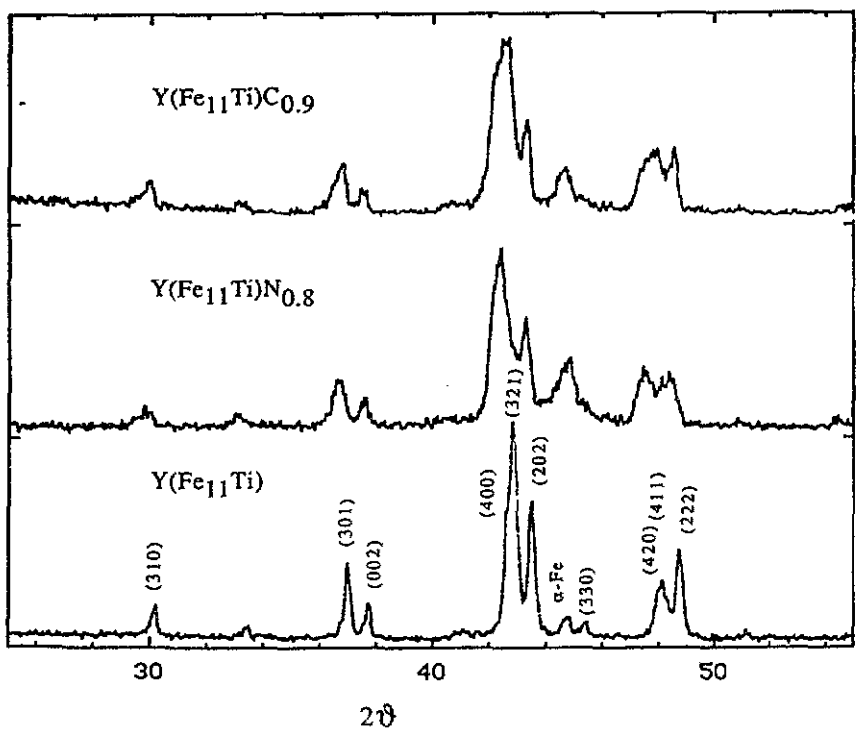

Figure 2. X-ray diffraction patterns of $Y(Fe_{11}Ti)$, $Y(Fe_{11}Ti)N_{1-\delta}$ and $Y(Fe_{11}Ti)C_{1-\delta}$.

2. Experimental results

The preparation and characterization of the $R(Fe_{11}Ti)$ samples have been fully discussed in I, Figure 2 shows x-ray diffraction patterns of $Y(Fe_{11}Ti)$, as well as samples

carbonated in butane or nitrogenated in nitrogen gas by heating powders for 2 h at $\simeq$ 500 °C. All are shown to be single-phase with the tetragonal $ThMn_{12}$ structure, except for the presence of some α-Fe (< 3%) in the carbide and nitride. Reduction in intensity of the iron peak on regrinding the carbide or nitride powders shows that this is mostly located on the particles' surface. Lattice parameters are listed in table 1.

Table 1. Structural and magnetic properties for $YFe_{11}Ti$ and $Y(Fe_{11}Ti)Z_{1-\delta}$ (Z = C, N) compounds.

Compound	a (Å)	c (Å)	V (Å^3)	$\Delta V/V$ (%)	T_c (K)	M (μ_B FU^{-1})
$YFe_{11}Ti$	8.505	4.800	347.2	—	524	19.0
$Y(Fe_{11}Ti)C_{0.9}$	8.580	4.798	353.2	1.73	678	21.6
$Y(Fe_{11}Ti)N_{0.8}$	8.581	4.800	353.4	1.79	742	21.7

Magnetization was measured using a vibrating-sample magnetometer in an applied magnetic field B_0 of up to 5 T at 4.2 K. The satuation magnetization for the parent compound, carbide and nitride, deduced by extrapolation to $1/B_0^2 \rightarrow 0$, were 141.2 J T^{-1} kg^{-1} (19.0 μ_B FU^{-1}), 158.9 J T^{-1} kg^{-1} (21.6 μ_B FU^{-1}) and 160.2 J T^{-1} kg^{-1} (21.7 μ_B FU^{-1}) respectively. The anisotropy fields for $Y(Fe_{11}Ti)$, nitride and carbide, deduced from the magnetization curve of fixed powder, were 3.4 T (K_1 = 2.0 MJ m^{-3}), 2.5 T (K_1 = 1.4 MJ m^{-3}) and 2.3 T (K_1 = 1.3 MJ m^{-3}) at 4.2 K respectively. The Curie temperature, measured by thermomagnetic scans in a field of 5 mT, increased from 524 K for $Y(Fe_{11}Ti)$ to 678 K for $Y(Fe_{11}Ti)C_{0.9}$ or 742 K for $Y(Fe_{11}Ti)N_{0.8}$.

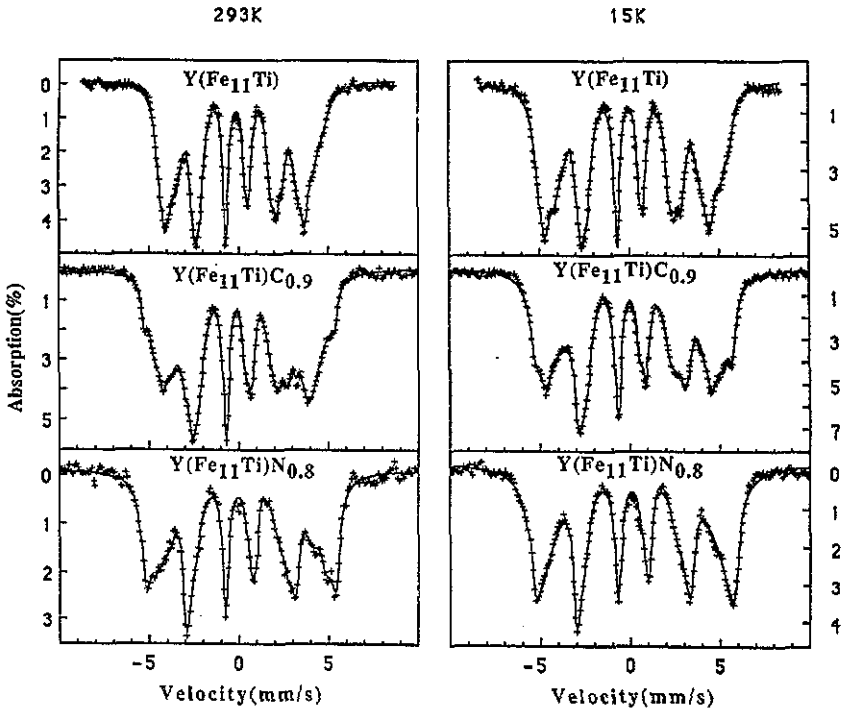

Figure 3. Mössbauer spectra of $Y(Fe_{11}Ti)Z_{1-\delta}$ at 293 K and at 15 K. The fits described are shown by the full lines.

Mössbauer spectra were recorded at 15 K and at room temperature using a conventional constant-acceleration spectrometer with a ^{57}Co source in a Rh matrix. A velocity calibration was made using the spectrum of an α-Fe absorber at room temperature. Samples consisted of 20 mg cm^{-2} of alloy powder mixed with icing sugar to form homogeneous and isotropic absorbers. Data are shown in figure 3. Fitting was done using five Lorentzian sextets with the intensity ratio 4:3:4 for the 8f, 8i and 8j sites. For both 8i and 8j sites two split subspectra with intensity 2:1 are due to the influence of Ti which occupies the 8i sites at random [18, 19]. The site symmetry is $m2m$ for 8i, 8j sites and $2/m$ for 8f sites [18]. Different linewidths were used for the outer, middle and inner lines of each sextet; they range from 0.15 to 0.50 mm s^{-1} full width at half maximum. The fitting procedure was described in detail in [21]. Based on the coordination of the sites and the observation that early transition-metal neighbours reduce the iron hyperfine field sharply, whereas iron neighbours tend to increase it [20], it is generally agreed that the hyperfine field of iron at 8f sites (9 iron neighbours, 1 titanium neighbour and 2 yttrium neighbours) should be the smallest and that at 8i sites (11.75 iron neighbours, 1.25 titanium neighbours and 1 yttrium neighbour) should be the largest [21–23]. Allocation of the component subspectra in table 2 follows this order. The average hyperfine field at 15 K is little changed in the carbide, but it increases by 13% in the nitride (table 2, figure 3). The average isomer shift increases significantly from the parent compound to carbide to nitride, with the largest increase at 8j sites as shown in figure 4.

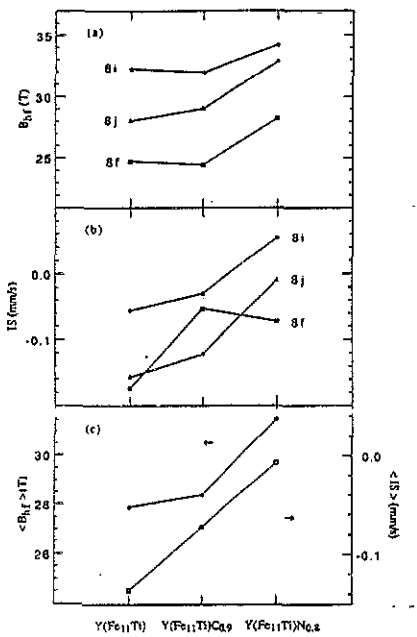

Figure 4. The (a) hyperfine fields and (b) isomer shifts at the three iron sites and (c) average hyperfine fields and isomer shifts for $Y(Fe_{11}Ti)$ and $Y(Fe_{11}Ti)Z_{1-\delta}$ (Z = C, N), measured at 15 K.

3. Electronic structure calculations

We recently applied the orthogonal linear combination of atomic orbitals (OLCAO) method to calculate the spin-polarized band structure of $Y(Fe_{11}Ti)$ and $Y(Fe_{11}Ti)N$

Table 2. Hyperfine fields for each crystallographic site of $YFe_{11}Ti$ and $Y(Fe_{11}Ti)Z_{1-\delta}$ (Z = C, N) deduced from ^{57}Fe Mössbauer spectra.

Compound	Temperature (K)	8i	8j	8f	$\langle B_{hf} \rangle$ (T)
$YFe_{11}Ti$	15	32.2	28.0	24.7	27.9
	293	27.1	23.9	20.8	23.6
$Y(Fe_{11}Ti)C_{0.9}$	15	31.9	29.0	24.4	28.1
	293	28.9	24.9	21.1	25.1
$Y(Fe_{11}Ti)N0.8$	15	34.2	32.8	28.2	31.5
	293	32.9	29.9	25.1	29.0

[12]. Details of the method of calculation, which is non-self-consistent, but uses Gaussian-type orbitals, are given elsewhere. Here we extend the calculations to $Y(Fe_{11}Ti)C$, and compare all the results. Results are available for $Y(Fe_{11}Ti)$ with the normal ($a = 0.855$ nm, $c = 0.475$ nm) and expanded ($a = 0.864$ nm, $c = 0.484$ nm) lattice parameters, and for the carbide and nitride with the expanded parameters. These are slightly different from the experimental values, but they are chosen to distinguish clearly the effect of volume expansion and the chemical effect of the interstitial atoms. Total and partial densities of states for carbide are shown in figure 5 and table 5 lists the numbers of electrons occupying the majority and minority sub-bands for each inequivalent crystallographic site of $Y(Fe_{11}Ti)C$. From the position of the Fermi level in the $\downarrow$ sub-band, the compound is clearly a weak ferromagnet. Hybridization with the carbon orbitals is evident in the structure near -7 eV for the 8j site, which is the direct neighbour of the interstitial carbon. The 2b interstitial site is coordinated by an octahedron of 2Y and 4Fe(8j), as shown in figure 1.

Calculated moments on the various sites as well as the total magnetization per formula unit and average iron moment are listed in table 3 for the parent compound in normal and expanded forms, as well as the carbide and the nitride. The calculation yields small positive moments, $\sim 0.1\ \mu_B$, for Y, Ti, C and N.

4. Discussion

4.1. Bulk magnetization

We first discuss the 3d magnetization of $Y(Fe_{11}Ti)Z_{1-\delta}$ (Z = C, N) intermetallics in terms of the magnetic valence model of Williams *et al* [24], which is a simple way of taking into account the effect of alloying on the magnetic moment assuming strong ferromagnet. The magnetic valence of an atom Z_m is defined as $2N_{d\uparrow}-Z_c$, where $N_{d\uparrow}$ is 5 for late 3d elements (Fe) and 0 for the early transition elements (Y, Ti), and Z_c is the chemical valence (3 for Y, 4 for Ti and C, 5 for N and 8 for Fe). The average moment per atom is then $\langle m \rangle = \langle Z_m \rangle + 2N_{sp\uparrow}$ where $\langle Z_m \rangle$ is the average magnetic valence per atom and N_{sp} is the occupancy of the unpolarized sp band, typically 0.3. For the parent compound, the carbide and the nitride, the model yields moments of 22.8, 19.4 and 18.4 μ_B FU^{-1} respectively. The value of 22.8 μ_B FU^{-1} for $Y(Fe_{11}Ti)$ is somewhat greater than that measured by extrapolating data on free powder to $1/B_0^2 = 0$ (19.0 μ_B FU^{-1}) or that calculated by the OLCAO method (20.3 μ_B FU^{-1}) [12]. These discrepancies arise because the 3d$\uparrow$ states are not completely full in $Y(Fe_{11}Ti)$ which is therefore a weak, not a strong ferromagnet.

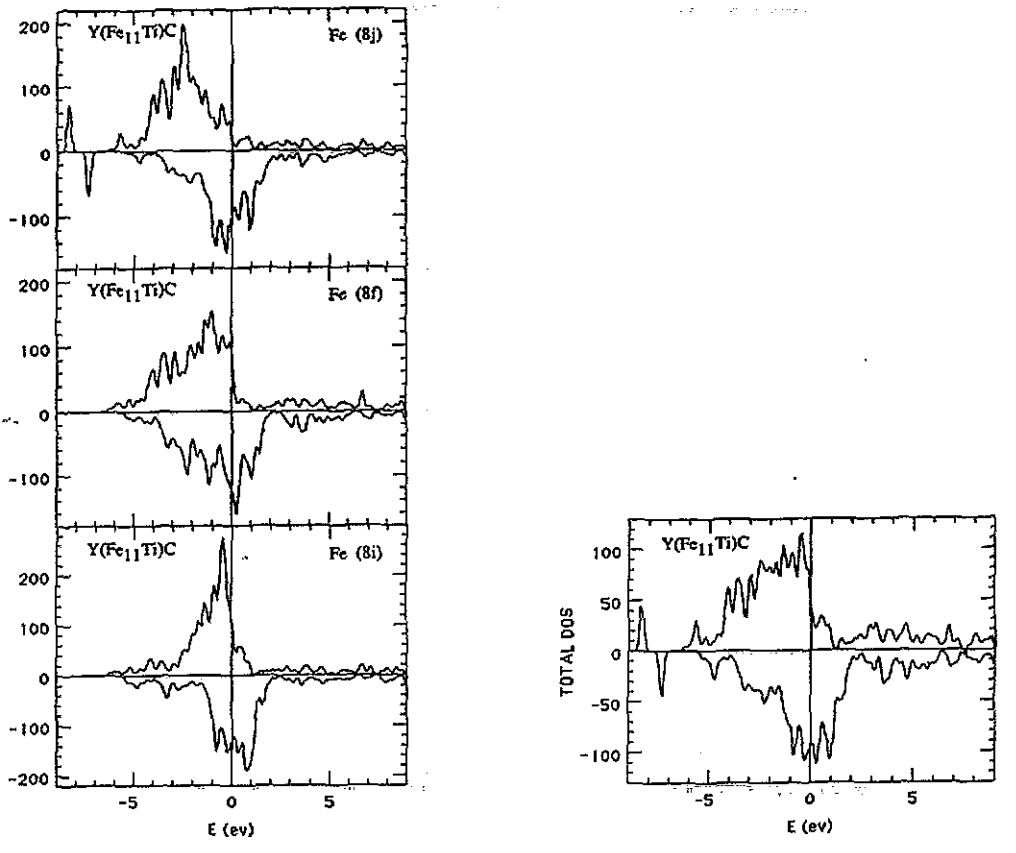

Figure 5. Total and partial densities of states for $Y(Fe_{11}Ti)C$ calculated by the OLCAO method.

The moments of 19.4 μ_B and 18.4 μ_B given for carbide and nitride by the magnetic valence model are evidently much smaller than the observed values (table 1). These compounds are also shown to be weak ferromagnets by electronic structure calculations with both 3d↑ and 3d↓ states lying at Fermi level. The reason for the failure of the model is that the assumption of a common band structure with a small N_{sp} occupancy is not valid for the interstitial compounds, where the nitrogen or carbon electrons must be considered in a separate atomic level some 8 eV below E_F (see figure 5). The situation is the same as for interstitial compounds with the 2:17 structure [7].

The volume expansion of the carbide (1.7%) and nitride (1.8%) are virtually identical, and the increase magnetic moment is 14% for both carbide and nitride. The increase of the spontaneous magnetization is essentially related to a narrowing of the 3d band due to volume expansion. It is not due to the presence of the interstitial atoms as such. In fact, calculations at constant volume (table 3) indicate that the chemical effect of the nitrogen or carbon interstitials is actually to reduce the iron moment slightly.

The average hyperfine field increases by 12% for nitride, but there is little change (1%) for the carbide (tables 1 and 2) although they have the same volume expansion. A similar effect was found in $Y_2Fe_{17}Z_{3-\delta}$ [7].

Table 3. Comparison of the magnetic moments in (*a*) $YFe_{11}Ti$, (*b*) $YFe_{11}Ti$ (expanded), (*c*) $Y(Fe_{11}Ti)C$, (*d*) $Y(Fe_{11}Ti)N$ and (*e*) hypothetical YFe_{12}.

Methods	T (K)	Y(2a) (μ_B/atom)	Fe(8f) (μ_B/atom)	Fe(8i) (μ_B/atom)	Fe(8j) (μ_B/atom)	T(8i) (μ_B/atom)	Z(2b) (μ_B/atom)	m_{Fe} (μ_B/Fe)	M (μ_B FU^{-1})	Reference
(*a*) Mössbauer	15	—	1.56	2.04	1.77	—	—	1.76	19.0	This work
Neutron diffraction	300	—	1.80	1.92	2.28	—	—	2.01	22.1	[19]
Calculated	—	0.27	1.77	1.91	1.76	0.21	—	1.80	20.3	[12]
(*b*) Calculated	—	0.26	1.88	2.01	1.87	0.18	—	1.91	21.5	[12]
(*c*) Mössbauer	15	—	1.73	2.26	2.06	—	—	2.00	21.6	This work
Calculated	—	0.17	1.59	2.06	1.71	0.21	0.21	1.76	19.7	This work
(*d*) Mössbauer	15	—	1.80	2.18	2 09	—	—	2.01	21.7	This work
Neutron diffraction	300	—	2.18	2.28	2.80	—	—	2.43	26.8	[28]
Neutron diffraction	300	—	1.90	2.16	2.10	—	—	2.04	22.5	[31]
Calculated	—	0.19	1.73	2.31	1.57	0.15	0.10	1.83	20.6	[12]
(*e*) Calculated	—	—	1.86	2.32	2.26	—	—	2.15	23.4	[38]
Extrapolated	—	—	1.78	2.32	2.18	—	—	2.07	22.8	[30]

Table 4. Magnetic moments and hyperfine fields in $Y(Fe_{11}Ti)$ and $Y(Fe_{11}Ti)Z_{1-\delta}$ (Z = C, N).

Compound	m (μ_B FU^{-1})	m_{Fe} (μ_B/Fe)	B_{hf} (T)	B_{cp} (T)	B_{4s} (T)	B_{orb} (T)	B_{hf}/m_{Fe} (T/μ_B)
$Y(Fe_{11}Ti)$	19.0	1.76	−27.9	−19.5	−9.4	1.0	−15.8
$Y(Fe_{11}Ti)C_{1-\delta}$	21.6	2.00	−28.1	−22.6	−6.5	1.0	−14.1
$Y(Fe_{11}Ti)N_{1-\delta}$	21.7	2.01	−31.5	−22.7	−9.5	1.0	−15.7

The hyperfine field may be written as

$$B_{hf} = B_{cp} + B_{4s} + B_{orb}$$

The main contributions to B_{hf} are the core polarization contribution B_{cp} from 1s, 2s and 3s core electrons, which is accurately proportional to the 3d moment with a constant conversion factor of $-11.3\ T/\mu_B$ [25] and the contribution from polarization of 4s electrons B_{4s}. A third term B_{orb} is due to the small orbital moment of iron, which typically of order 0.1 μ_B. The proportionality factor here is 42 T/μ_B [25]. Table 4 lists magnetic moments and hyperfine fields in $Y(Fe_{11}Ti)$ and $Y(Fe_{11}Ti)Z$ (Z = C, N), including the contributions B_{cp}, B_{4s} and B_{orb}. The anisotropic orbital term B_{orb} is deduced experimentally to be 1.0 T by comparing the average hyperfine field at 15 K in $Ho(Fe_{11}Ti)$, where the magnetization lies along the c-axis, with that in $Dy(Fe_{11}Ti)$, where the magnetization lies in the c-plane. The orbital moment is assumed to be unchanged in the nitride and carbide. Table 4 shows that the low hyperfine field in the carbide is due to a low 4s contribution; B_{4s} includes the effect of polarization of the atomic 4s electrons and the transferred hyperfine field from neighbouring atoms.

Table 5. Values of the number of electrons occupying the majority sub-band, $Q^{\uparrow}$, and the minority sub-band, $Q_{\downarrow}$, for each inequivalent crystallographic site of $Y(Fe_{11}Ti)C$. The magnetic moment is defined as $\mu = Q^{\uparrow} - Q_{\downarrow}$, in units of μ_B, and total electron number is given by $Q = Q^{\uparrow} + Q_{\downarrow}$.

	Y	Fe(8j)	Fe(8f)	Fe(8i)	Ti	C
$Q^{\uparrow}$	1.695	5.085	4.995	4.762	1.405	1.744
$Q_{\downarrow}$	1.531	3.382	3.409	2.707	1.195	1.537
Q	3.226	8.467	8.404	7.469	2.600	3.281
μ	0.164	1.703	1.586	2.055	0.210	0.207

Total majority electrons	=	118.90
Total minority electrons	=	79.10
Total electrons	=	198
Magnetization	=	19.9 μ_B FU^{-1}
Average Fe moment	=	1.76 μ_B

It is often assumed that hyperfine fields are proportional to the 3d magnetization. Frequently used proportionality factors derived experimental results are $-15.6\ T/\mu_B$ for intermetallic compounds with the 1:12 structure and $-14.8\ T/\mu_B$ for intermetallic compounds with the 2:17 structure [26]. Coehoorn pointed out that the use of constant conversion factors can lead to errors of about 0.3 μ_B in estimates of the moments from the hyperfine fields [3]. We found that for $Y_2Fe_{17}Z_{3-\delta}$ the relation between average iron moment and average hyperfine field is $\simeq -15.3\ T/\mu_B$ in Y_2Fe_{17}, the hydride and nitride, but $-14.1\ T/\mu_B$ in the carbide [7]. The conversion factors at different sites vary from $-13.5\ T/\mu_B$ to $-17.3\ T/\mu_B$. For $Y(Fe_{11}Ti)$, carbide and nitride the situation seems to be similar. The conversion factor is essentially the same in the pure compound and nitride, but it is significantly less in the carbide due to the transferred hyperfine field (table 4).

Table 6. Volume dependence of Curie temperature and magnetization.

Compound	Density of states at E_F (states eV^{-1}/Fe atom)		Magnetic moment (μ_B/Fe atom)		Stoner parameter (eV)	T_c[Y(Fe_{11}Ti)Z]/T_c[Y(Fe_{11}Ti)]		$\delta \ln M/\delta \ln V$ (μ_B/Fe atom)	
	Spin up	Spin down	Exp.	Cal.		Exp.	Cal.	Exp.	Cal.
Y(Fe_{11}Ti)	0.19	0.62	1.76	1.80	0.95	1	1	—	—
Y(Fe_{11}Ti)C	0.29	0.48	2.00	1.76	0.93	1.29	0.68	7.9	0.84
Y(Fe_{11}Ti)N	0.32	0.49	2.01	1.83	0.93	1.42	0.67	7.9	0.94

4.2. Local magnetization and hyperfine field

Table 3 summarizes the results of local moments in $Y(Fe_{11}Ti)$, carbide and nitride obtained from Mössbauer spectroscopy, neutron diffraction and electronic structure calculation, including calculation results on the expanded parent compound and hypothetical YFe_{12}. No neutron diffraction results on $Y(Fe_{11}Ti)C$ have been reported so far. For comparison we use the conversion factor given in table 4 to get a local moment from the ^{57}Fe hyperfine field at the three sites.

In general the iron moments are sensitive to local coordination and nearest-neighbour distances. Iron neighbours increase the iron moment and yttrium neighbours reduce it. The neutron diffraction results of Moze *et al* [18], Yang *et al* [19] and Helmhodt *et al* [27] have established that a quarter of 8i sites are occupied by Ti atoms. According to the crystal structure of $Y(Fe_{11}Ti)$ the 8i site has 11.75 iron nearest neighbours on average, whereas each 8j and 8f site has only 9.0. The average Fe–Fe distances are 2.723 Å (8i), 2.579 Å (8j) and 2.500 Å (8f) obtained by Moze *et al*, 2.697 Å (8i), 2.564 Å (8j) and 2.488 Å (8f) by Helmholdt *et al*, 2.713 Å (8i), 2.594 Å (8j) and 2.518 Å (8f) by Yang *et al*, all following the relation $d_{Fe-Fe}(8i) > d_{Fe-Fe}(8j) > d_{Fe-Fe}(8f)$. One yttrium nearest-neighbour for an 8i site but two for 8j and 8f sites also indicates that the order $\mu_{Fe}(8i) > \mu_{Fe}(8j) > \mu_{Fe}(8f)$ should be reasonable. Most band calculations for Y–Fe compounds with the 1:12 structure support this view. Average Fe–Fe distances in the nitride follow the same order as pure $Y(Fe_{11}Ti)$ [28]. From these considerations the order $B_{hf}(8i) > B_{hf}(8j) > B_{hf}(8f)$ was used to identify the components of the fits to the Mössbauer spectra of $Y(Fe_{11}Ti)$, carbide and nitride. Almost all other authors adopt this order [22, 29, 30], although different numbers of subspectra were needed in order to obtain a good fit to the Mössbauer data.

Table 7. Anisotropy constant K_1 (in MJ m^{-3}) and anisotropy field (in T) for the Fe sublattice in $Y(Fe_{11}Ti)$ and $Y(Fe_{11}Ti)Z_{1-\delta}$ at 4.2 K.

$Y(Fe_{11}Ti)$		$Y(Fe_{11}Ti)C_{1-\delta}$		$Y(Fe_{11}Ti)N_{1-\delta}$	
K_1	B_a	K_1	B_a	K_1	B_a
2.0(1)	3.4(3)	1.4(2)	2.5(3)	1.3(2)	2.3(3)

The average isomer shift increases from -0.136 mm s^{-1} for $Y(Fe_{11}Ti)$, to -0.072 mm s^{-1} for carbide to -0.015 mm s^{-1} for nitride as shown in figure 4. Assuming that the number of electrons in the 3d–4s conduction band of iron is a constant, the pure volume effect on the iron isomer shift $\Delta IS/\Delta \ln V$ is expected to be 1.3 mm s^{-1} for the close-packed structure corresponding to the isomer-shift parameter $\alpha = -0.27\ a_0^3$ mm s^{-1} [32], whereas observed values are 3.7 mm s^{-1} for carbide and 6.7 mm s^{-1} for nitride. This suggests that electron transfer is larger in nitride than in carbide, and that 4s → 2p interatomic charge transfer may be the main process because a value of $\Delta IS/\Delta \ln V$ of more than 3 would mean that interatomic charge transfer from 4s to 3d exceeded 0.5 electrons, which seems not to be possible [33]. The situation is different in $R_2Fe_{17}Z_{3-\delta}$, where the value of $\Delta IS/\Delta \ln V$ is 1.8 mm s^{-1} for nitride and only 0.7 mm s^{-1} for carbide which suggests that interband charge transfer occurs in the opposite sense in nitride and carbide [34].

4.3. Volume effects on the Curie temperature and magnetization

According to the Stoner model [35] and the spin-fluctuation theory of Mohn and Wohlfarth [36], the Curie temperature is given by

$$T_c^2/T_{st}^2 + T_c/T_{sf} - 1 = 0.$$

Neglecting the first term, which contains the inverse of the square of the Stoner Curie temperature, and considering only T_{sf}, which is a characteristic temperature describing the influence of spin fluctuations, given by $T_{sf} = m_0^2(10k_B\chi_0)^{-1}$, we get a simple expression

$$T_c = T_{sf} = m_0^2(10k_B\chi_0)^{-1}$$

where m_0 is the magnetic moment, k_B is the Boltzmann constant and

$$\chi_0^{-1} = [1/(2N^{\uparrow}(E_F)) + 1/(2N_{\downarrow}(E_F)) - I]/2\mu_B^2$$

where $N^{\uparrow}$ and $N_{\downarrow}$ are up-spin and down-spin densities of states at the Fermi level is the Stoner parameter which is 0.95 eV for $Y(Fe_{11}Ti)$.

The volume dependence of the magnetization, neglecting the elastic term, is described by [37]

$$V\,\delta M/\delta V = \tfrac{5}{3}Im_0[1/(2N^{\uparrow}(E_F)) + 1/(2N_{\downarrow}(E_F)) - I]^{-1}.$$

Table 6 lists both the values of the T_c ratios, $T_c[Y(Fe_{11}Ti)Z]/T_c[Y(Fe_{11}Ti)]$, and $\delta \ln M/\delta \ln V$ deduced from our electronic structure calculation and the experimental results. The agreement between experiment and calculation is poor. This probably reflects the difficulty in locating the Fermi level precisely in the non-self-consistent OCLAO calculation. The value of $N^{\uparrow}(E_F)$ in particular is extremely sensitive to tiny changes in the position of E_F (see figure 5).

4.4. Anisotropy

The magnetocrystallic anisotropy is associated with the small 3d orbital moment. It is very difficult to calculate accurately. The decrease in K_1 in carbide and nitride (table 7) can be due to a change in the 3d orbital moment, or the change in crystal field introduced by the interstitial.

5. Conclusions

The $Y(Fe_{11}Ti)$ compound and the interstitial nitride and carbide are all weak ferromagnets. Nevertheless the ↑ sub-band is almost full, and the magnetization is close to the value of 22.8 μ_B FU^{-1} expected for strong ferromagnetism.

The increase of magnetization in the interstitial compounds is essentially due to the volume expansion. The chemical effect of N or C is to reduce the iron moment slightly by hybridization, especially on 8i sites.

An increase in hyperfine field commensurate with moment change is observed in the nitride, but not in the carbide. This may be due to different 4f transferred hyperfine fields.

The increase in Curie temperature in the interstitial compounds is not reproduced by the electronic structure calculation because of the great sensitivity of the $N^{\uparrow}(E_F)$ density of states to the exact position of the Fermi level.

Acknowledgments

This work forms part of the Concerted European Action on Magnets. It was supported by the BRITE/EURAM programme of the European Commission. We are grateful to D P F Hurley for making some samples and to Justin Lawler for help on the magnetization measurements at low temperature.

References

[1] Inoue J and Shimizu M 1985 *J. Phys. F: Met. Phys.* **15** 1511
[2] Coehoorn R 1989 *Phys. Rev.* B **39** 13072
[3] Coehoorn R 1991 *J. Magn. Magn. Mater.* **99** 55
[4] Coey J M D and Sun H 1990 *J. Magn. Magn. Mater.* **87** L251
[5] Sun H, Coey J M D, Otani Y and Hurley D P F 1990 *J. Phys.: Condens. Matter* **2** 6465
[6] Coey J M D, Sun H, Otani Y and Hurley D P F 1991 *J. Magn. Magn. Mater.* **98** 76
[7] Qi Q-N, Sun H, Skomski R and Coey J M D 1992 *Phys. Rev.* B **45** 12278
[8] Nikitin S A, Tishin A M, Kuz'min M D and Spichkin Y I 1991 *Phys. Lett.* **153A** 155
[9] Li Y-P, Li H-S and Coey J M D 1991 *Phys. Status Solidi* b **166** K107
[10] Jaswal S S, Yelon W B, Hadjipanayis G C, Wang Y Z and Sellmyer D J 1991 *Phys. Rev. Lett.* **67** 644
[11] Li Y-P and Coey J M D 1992 *Phys. Rev.* B submitted
[12] Li Y-P and Coey J M D 1992 *Solid State Commun.* **81** 447
[13] Hurley D P F and Coey J M D 1992 *J. Phys.: Condens. Matter* **4** 5573
[14] Yang Y-C, Zhang X-D, Ge S-L, Pan Q, Kong L-S, Li H-L, Yang J-L, Zhang B-S, Ding Y-F and Ye C-T 1991 *J. Appl. Phys.* **70** 6001
[15] Liao L-X, Altounian Z and Ryan D H 1991 *J. Appl. Phys.* **70** 6006
[16] Coey J M D 1991 *Physica Scr.* T **39** 21
[17] Yang Y-C, Zhang X-D, Kong L-S, Pan Q, Yang J-L, Ding Y-F, Zhang B-S, Ye C-T and Jin L 1991 *Solid State Commun.* **78** 317
[18] Moze O, Pareti L, Solzi M and David W I F 1988 *Solid State Commun.* **66** 465
[19] Yang Y-C, Sun H, Kong L-S, Yang J-L, Ding Y-F, Zhang B-S, Ye C-T, Jin L and Zhou H-M 1988 *J. Appl. Phys.* **64** 5968
[20] Coey J M D 1991 *Science and Technology of Nonostructured Magnetic Materials* ed G C Hadjipanayis and G A Prinz (New York: Plenum) p 439
[21] Hu B-P, Li H-S and Coey J M D 1989 *Hyperfine Interact.* **45** 233
[22] Deriu A, Leo G, Moze O, Pareti L, Solzi M and Xue R H 1989 *Hyperfine Interact.* **45** 241
[23] Li Z-W, Zhou X-Z, Morrish A H and Yang Y-C 1990 *J. Phys.: Condens. Matter* **2** 4253
[24] William A R, Moruzzi V L, Malozemoff A P and Terakura K 1983 *IEEE Trans. Magn.* **MAG-19** 1983
[25] Coehoorn R, Denissen C J N and Eppenga R 1991 *J. Appl. Phys.* **69** 6222
[26] Gubbens P C M, van Apeldorn J H J, van der Kraan A M and Buschow K H J 1974 *J. Phys. F: Met. Phys.* **4** 921
[27] Helmhodt R B, Vleggaar J J and Buschow K H J 1988 *J. Less-Common Met.* **138** 111
[28] Yang Y-C, Zhang H-D, Kong L-S and Pan Qi 1991 *Solid State Commun.* **78** 313
[29] Li Z-W, Zhou X-Z and Morrish A H 1991 *J. Appl. Phys.* **69** 5602
[30] Denissen C J M, Coehoorn R and Buschow K H J 1990 *J. Magn. Magn. Mater.* **87** 51
[31] Yang Y-C, Zhang X-D, Ge S-L, Pan Q, Kong L-S, Li H-L, Yang J-L, Zhang B-S, Ding Y-F and Ye C-T 1991 *J. Appl. Phys.* **70** 6001
[32] Moyzis Jr J A and Drickamer H G 1968 *Phys. Rev.* **171** 389
[33] Williamson D L 1978 *Mössbauer Isomer Shifts* ed G K Shenoy and F E Wagner (Amsterdam: North-Holland)
[34] Qi Q-N, Sun Hong and Coey J M D 1991 *Hyperfine Interact.* **68** 27
[35] Gunnarson O 1976 *J. Phys. F: Met. Phys.* **6** 587
[36] Mohn P and Wohlfarth E P 1987 *J. Phys. F: Met. Phys.* **17** 2421
[37] Coehoorn R 1991 *Supermagnets, Hard Magnetic Materials* ed G J Long and P Grandjean (Amsterdam: Kluwer Academic) p 133
[38] Coehoorn R 1990 *Phys. Rev.* B **41** 11790